Received October 2002
Revised October 2002
Accepted January 2003

Natural convection flows in complex cavities by BEM

L. Škerget, M. Hriberšek and Z. Žunič
Faculty of Mechanical Engineering, Institute of Power, Process and Environmental Engineering, University of Maribor, Maribor, Slovenia

Keywords *Boundary elements methods, Differential equations, Convection, Fluid dynamics*

Abstract *A numerical method for the solution of the Navier-Stokes equations is developed using an integral representation of the conservation equations. The velocity-vorticity formulation is employed, where the kinematics is given with the Poisson equation for a velocity vector, while the kinetics is represented with the vorticity transport equation. The corresponding boundary-domain integral equations are presented along with discussions of the kinetics and kinematics of the fluid flow problem. The boundary-domain integral formulation is developed and tested for natural convection flows in closed cavities with complex geometries.*

1. Introduction

The research field of natural convection in closed cavities has gained an increased attention due to many practical situations, where natural convection phenomena plays a dominant role. In thermal engineering, natural convection is one of the most important heat transfer mechanisms, especially in closed cavities, as for example in building elements, seals of cooling appliances and thermal storage tanks.

The main driving force of fluid motion in the case of natural convection is the density change due to temperature increase or decrease. If we deal with cavity with a horizontal temperature difference, such induced fluid motion can strongly affect the overall heat transfer across the cavity. If the working fluid is known, the only way to influence heat transfer is to change the geometry the cavity. This leads to cavities with complex geometries, where usually no known correlations for heat transfer coefficient exists. Numerical investigation of such heat and fluid flow phenomena is therefore of great importance, as it gives an accurate insight into heat and flow conditions inside the cavity. Several researchers already published numerical results on natural convection in complex geometries, predominantly by the use of finite difference method (Chang and Tsay, 2001; Ciofalo and Karayiannis, 1991).

In the present work, the main attention will be on the development of an accurate boundary element algorithm for computation of natural convection flows in complex geometries. Among different approximation methods developed the boundary element method has proved to be very accurate for the computation of heat transfer in solids as well as in fluids at moderate Ra number values. Since in real life problems, high value Ra flows frequently occur, heat convection starts to play a predominant role. In such cases, the

International Journal of Numerical Methods for Heat & Fluid Flow
Vol. 13 No. 6, 2003
pp. 720-735

0961-5539
DOI 10.1108/09615530310498394

classical boundary element formulations are not suitable for computations anymore. However, in the last few years, a lot of work has been done on the further development of BEM algorithms for natural convection flows, among others (Hribersek and Kuhn, 2000; Skerget *et al.*, 1989, 1999).

Several numerical issues have to be solved in order to construct an accurate and conservative numerical method. With higher values of Ra number, accurate prediction of convection phenomena becomes extremely important, as well as capturing high gradients in the viscous sublayer. In general, conservation of mass and energy has to be preserved in order to obtain physically relevant solutions.

This paper presents a detailed derivation of a conservative boundary element algorithm in the form of boundary-domain integral method. Since the solution to nonisothermal Navier-Stokes equations is done through the velocity-vorticity approach, a special attention is devoted to conservation of mass and vorticity in the computational domain, as this is the key issue in obtaining accurate solutions in complex geometry flows. Additionally, the derivation of integral form of flow kinematics equation starting from the velocity-vector flow kinematics equation, developed by Skerget *et al.* (1999), is described, leading to integral form of flow kinematics formally equal to vector potential flow kinematics (Hribersek and Skerget, 1996; Skerget *et al.*, 1989; Wu, 1982; Wu and Thompson, 1973).

2. Navier-Stokes equations

The analytical description of the motion of a continuous medium is based on the conservation of mass, momentum and energy, and the associated equations of state and constitutive relations. With the assumptions of incompressibility within Boussinesq approximation, the following partial differential equations set can be stated in an indicial notation form for a right-handed Cartesian coordinate system

$$\frac{\partial v_j}{\partial x_j} = 0, \tag{1}$$

$$\frac{Dv_i}{Dt} = -\frac{1}{\rho}\frac{\partial P}{\partial x_i} + \nu \frac{\partial^2 v_i}{\partial x_j \partial x_j} + F_B g_i, \tag{2}$$

$$\frac{DT}{Dt} = a \frac{\partial^2 T}{\partial x_j \partial x_j}, \tag{3}$$

where the vector field functions v_i, g_i, and x_i are, respectively, velocity, gravity and position. The scalar quantities $P = p - \rho g_j r_j$ and T are modified pressure and temperature, while D/Dt represents the Stokes derivative. The material

properties such as mass density ρ, specific isobaric heat c_p, kinematic viscosity, ν and heat conductivity, λ are assumed to be constant parameters. In the heat transport equation, $a = \lambda/(\rho c_p)$ denotes the thermal diffusivity.

In the case of Boussinesq approximation, the normalised density--temperature variation function, F_B can be written as follows

$$F_B = -\beta_T(T - T_o), \tag{4}$$

where β_T is a thermal volume expansion coefficient and T_o is the reference temperature.

The Navier-Stokes equation set for nonisothermal fluid flow consists of equations (1)-(3), which present the basis for the determination of velocity, pressure and temperature field functions, provided that adequate initial and boundary conditions are prescribed.

3. Kinematics and kinetics of incompressible flow

The dynamics of a viscous incompressible fluid is partitioned into its kinematic and kinetic aspect through the use of derived vector vorticity field function $\omega_i(r_j, t)$ obtained as a curl of the compatibility velocity field $v_i(r_j, t)$

$$\omega_i = e_{ijk}\frac{\partial v_k}{\partial x_j}, \quad \frac{\partial \omega_i}{\partial x_j} = 0, \tag{5}$$

which is solenoidal vector by the definition, and e_{ijk} is the permutation unit tensor.

By applying the curl operator to the vorticity definition

$$\vec{\nabla} \times \vec{\omega} = \vec{\nabla} \times (\vec{\nabla} \times \vec{v}) = \vec{\nabla}(\vec{\nabla} \cdot \vec{v}) - \nabla^2 \vec{v} \tag{6}$$

and by using the continuity equation for the incompressible flows, $\vec{\nabla} \cdot \vec{v} = 0$, the following vector elliptic Poisson equation for velocity vector is obtained

$$\nabla^2 \vec{v} + \vec{\nabla} \times \vec{\omega} = 0. \tag{7}$$

Equation (7) represents the kinematics of an incompressible fluid motion, expressing the compatibility and restriction conditions between velocity and vorticity field functions. With either equations (1) and (5), or (7), the kinematics of the fluid motion problem is governed by a linear set of elliptic differential equations. Since equation (7) is elliptic, the correct boundary condition to prescribe is either Dirichlet's or Neuman's or a linear combination of the two, over the entire boundary Γ.

The kinetic aspect is governed by the parabolic diffusion-convection vorticity transport equation obtained by applying the curl operator to the momentum equation (2),

$$\frac{D\omega_i}{Dt} = \frac{\partial\,\omega_j v_i}{\partial x_j} + \nu\,\frac{\partial^2 \omega_i}{\partial x_j \partial x_j} + e_{ijk} g_k\,\frac{\partial F_B}{\partial x_j}. \tag{8}$$

For the case of the two-dimensional flow, the vorticity vector has just one component, perpendicular to the plane of the flow. Thus, the twisting-stretching term is identical to zero $(\vec{\omega}\cdot\vec{\nabla})\vec{v} = 0$, simplifying equation (8) to a scalar transport equation for vorticity

$$\frac{D\omega}{Dt} = \nu\,\frac{\partial^2 \omega}{\partial x_j \partial x_j} + e_{ij} g_j\,\frac{\partial F_B}{\partial x_i}, \tag{9}$$

e_{ij} being the permutation unit symbol. The vorticity transport equation is nonlinear due to the product of velocity and vorticity, which are kinematically dependent variables. Due to the buoyancy source term, the vorticity transport equation is also coupled to the energy equation, making the nonlinearity of the equations set even more severe.

4. Integral representations

The unique advantage of the boundary element method originates from the application of Green fundamental solutions as particular weighting functions. Since they only consider the linear transport phenomenon, an appropriate selection of a linear differential operator $\mathscr{L}[\cdot]$ is of main importance in establishing a stable and accurate singular integral representations corresponding to original differential conservation equations.

All different conservation models can be written in the following general form

$$\mathscr{L}[u] + b = 0, \tag{10}$$

where the operator $\mathscr{L}[\cdot]$ can be either elliptic or parabolic, $u(r_j, t)$ is an arbitrary field function, and the nonhomogeneous term $b(r_j, t)$ is applied for nonlinear transport effects or pseudo body forces.

4.1 Integral representations for flow kinematics

The velocity equation (7) can be recognized as a nonhomogeneous elliptic vector Poisson equation, thus employing the linear elliptic Laplace differential operator as follows

$$\mathscr{L}[\cdot] = \frac{\partial^2(\cdot)}{\partial x_j \partial x_j} \tag{11}$$

the following can be stated:

$$\mathscr{L}[v_i] + b_i = \frac{\partial^2 v_i}{\partial x_j \partial x_j} + b_i = 0 \tag{12}$$

The singular boundary integral representation for the velocity vector can be formulated by using the Green theorems for scalar functions, or weighting residuals technique, rendering the following vector integral formulation

$$c(\xi)\vec{v}(\xi) + \int_\Gamma \vec{v}\,\frac{\partial u^*}{\partial n}\,\mathrm{d}\Gamma = \int_\Gamma \frac{\partial \vec{v}}{\partial n} u^*\,\mathrm{d}\Gamma + \int_\Omega \vec{\nabla}\times\vec{\omega}\;\; u^*\,\mathrm{d}\Omega, \tag{13}$$

with u^* the elliptic Laplace fundamental solution. Using vector identities on the domain integral, the following integral representation can be written as

$$c(\xi)\vec{v}(\xi) + \int_\Gamma \vec{v}\,\frac{\partial u^*}{\partial n}\,\mathrm{d}\Gamma = \int_\Gamma \frac{\partial \vec{v}}{\partial n} u^*\,\mathrm{d}\Gamma - \int_\Gamma \vec{\omega}\times\vec{n}\;\; u^*\,\mathrm{d}\Gamma + \int_\Omega \vec{\omega} \times \vec{\nabla} u^*\,\mathrm{d}\Omega, \tag{14}$$

or in tensor notation form

$$c(\xi)v_i(\xi) + \int_\Gamma v_i\,\frac{\partial u^*}{\partial n}\,\mathrm{d}\Gamma = \int_\Gamma \frac{\partial v_i}{\partial n} u^*\,\mathrm{d}\Gamma - e_{ijk}\int_\Gamma \omega_j n_k u^*\,\mathrm{d}\Gamma + e_{ijk}\int_\Omega \omega_j\,\frac{\partial u^*}{\partial x_k}\,\mathrm{d}\Omega. \tag{15}$$

For plane flow situation, equation (15) reduces to the following two scalar equations, as follows

$$c(\xi)v_i(\xi) + \int_\Gamma v_i\,\frac{\partial u^*}{\partial n}\,\mathrm{d}\Gamma = \int_\Gamma \frac{\partial v_i}{\partial n} u^*\,\mathrm{d}\Gamma + e_{ij}\int_\Gamma \omega n_j u^*\,\mathrm{d}\Gamma - e_{ij}\int_\Omega \omega\,\frac{\partial u^*}{\partial x_j}\,\mathrm{d}\Omega. \tag{16}$$

One of the most important issues in numerical modeling of incompressible flow phenomena is to obtain divergence free final solution, as well as for mass conservation, equation (1), as for vorticity conservation, equation (5). In case of equations (7) or (14), it can be easily shown (Wu and Thompson, 1973) that it admits solutions where neither divergences are zero. Thus, equation (14) does not, in general, represent the kinematics of the incompressible fluid flow. However, in cases of flows in closed cavities, induced by natural convection phenomena, where the no-slip boundary condition is applied on the whole boundary, equation (14) may be used in the place of equations (1) and (5).

As we do not want the BEM numerical formulation of Navier-Stokes equations to be limited to some selected cases only, we will derive the integral representation of flow kinematics which will ensure divergence free solutions. Therefore, we will use additional compatibility and restriction conditions in

derivation of integral representations for the general fluid flow situation, where boundary Γ may be in the interior of the fluid.

Let us, for the sake of simplicity of derivation, focus on plane flow kinematics, given by equation (16). By using the relations for the normal velocity component derivatives

$$\begin{aligned} \frac{\partial v_x}{\partial n} &= \frac{\partial v_x}{\partial x} n_x + \frac{\partial v_x}{\partial y} n_y \\ \frac{\partial v_y}{\partial n} &= \frac{\partial v_y}{\partial x} n_x + \frac{\partial v_y}{\partial y} n_y, \end{aligned} \tag{17}$$

vorticity definition

$$\omega = \frac{\partial v_y}{\partial x} - \frac{\partial v_x}{\partial y}, \tag{18}$$

tangent and normal unit vectors

$$\begin{aligned} \vec{n} &= (n_x, n_y) \\ \vec{t} &= (t_x, t_y) = (-n_y, n_x), \end{aligned} \tag{19}$$

and by applying continuity equation (1), one can write the following relations

$$\begin{aligned} \frac{\partial v_x}{\partial x} n_x + \frac{\partial v_x}{\partial y} n_y + \frac{\partial v_y}{\partial x} n_y - \frac{\partial v_x}{\partial y} n_y &= -\frac{\partial v_y}{\partial t} \\ \frac{\partial v_y}{\partial x} n_x + \frac{\partial v_y}{\partial y} n_y - \frac{\partial v_y}{\partial x} n_x + \frac{\partial v_x}{\partial y} n_x &= \frac{\partial v_x}{\partial t}, \end{aligned} \tag{20}$$

thus the boundary integrals on the right hand side of equation (16) can be simplified, resulting in

$$c(\xi) v_i(\xi) + \int_\Gamma v_i \frac{\partial u^*}{\partial n} \, \mathrm{d}\Gamma = -\int_\Gamma \frac{\partial v_j}{\partial t} u^* \, \mathrm{d}\Gamma - e_{ij} \int_\Omega \omega \frac{\partial u^*}{\partial x_j} \, \mathrm{d}\Omega. \tag{21}$$

Then equation (21) can be further reformulated as

$$\begin{aligned} c(\xi) v_i(\xi) + \int_\Gamma v_i \frac{\partial u^*}{\partial n} \, \mathrm{d}\Gamma = \int_\Gamma v_j \frac{\partial u^*}{\partial t} \, \mathrm{d}\Gamma - e_{ij} \int_\Gamma \frac{\partial v_j u^*}{\partial t} \, \mathrm{d}\Gamma \\ - e_{ij} \int_\Omega \omega \frac{\partial u^*}{\partial x_j} \, \mathrm{d}\Omega, \end{aligned} \tag{22}$$

and by applying the Gauss theorem, the second boundary integral on the right hand side of the equation vanishes, resulting in the final integral representation for the two dimensional plane kinematics

$$c(\xi)v_i(\xi) + \int_\Gamma v_i \frac{\partial u^*}{\partial n}\,\mathrm{d}\Gamma = \int_\Gamma v_j \frac{\partial u^*}{\partial t}\,\mathrm{d}\Gamma - e_{ij}\int_\Omega \omega \frac{\partial u^*}{\partial x_j}\,\mathrm{d}\Omega, \qquad (23)$$

which is identical to the integral representation using the vector potential formulation for the flow kinematics (Hribersek and Skerget, 1996).

The general boundary integral representation can be easily stated as

$$c(\xi)\vec{v}(\xi) + \int_\Gamma (\vec{\nabla}u^* \cdot \vec{n})\vec{v}\,\mathrm{d}\Gamma = \int_\Gamma (\vec{\nabla}u^* \times \vec{n}) \times \vec{v}\,\mathrm{d}\Gamma + \int_\Omega (\vec{\omega} \times \vec{\nabla}u^*)\,\mathrm{d}\Omega, \qquad (24)$$

or in the compact symbolic notation form for the cyclic combination of indices $ijkij = 12312$,

$$\begin{aligned} c(\xi)v_i(\xi) + \int_\Gamma v_i \frac{\partial u^*}{\partial n}\,\mathrm{d}\Gamma = {} & \int_\Gamma v_k\left(\frac{\partial u^*}{\partial x_k}n_i - \frac{\partial u^*}{\partial x_i}n_k\right)\mathrm{d}\Gamma \\ & - \int_\Gamma v_j\left(\frac{\partial u^*}{\partial x_i}n_j - \frac{\partial u^*}{\partial x_j}n_i\right)\mathrm{d}\Gamma \\ & + \int_\Omega \omega_j \frac{\partial u^*}{\partial x_k}\,\mathrm{d}\Omega - \int_\Omega \omega_k \frac{\partial u^*}{\partial x_j}\,\mathrm{d}\Omega. \end{aligned} \qquad (25)$$

The boundary integral representation (24) is completely equivalent to equations (1) and (5), or equation (7), together with velocity boundary conditions expressing the kinematics of a general incompressible fluid flow in the integral form.

When the unknowns are the boundary vorticity values or the tangent velocity component values, one has to use the tangential component of the vector (equation (24))

$$\begin{aligned} & c(\xi)\vec{n}(\xi) \times \vec{v}(\xi) + \vec{n}(\xi) \times \int_\Gamma (\vec{\nabla}u^* \cdot \vec{n})\vec{v}\,\mathrm{d}\Gamma \\ & \quad = \vec{n}(\xi) \times \int_\Gamma (\vec{\nabla}u^* \times \vec{n}) \times \vec{v}\,\mathrm{d}\Gamma + \vec{n}(\xi) \times \int_\Omega (\vec{\omega} \times \vec{\nabla}u^*)\,\mathrm{d}\Omega \end{aligned} \qquad (26)$$

in order to obtain the appropriate nonsingular implicit system of equations. Then equation (26) enables boundary vorticity values to be expressed in integral form within the domain integral, excluding the need to use an approximate formulae for determining boundary vorticity values, which would bring an additional error in the computational scheme.

When the normal velocity components to the boundary are unknown, the normal form has to be employed:

$$c(\xi)\vec{n}(\xi)\cdot\vec{v}(\xi)+\vec{n}(\xi)\cdot\int_{\Gamma}(\vec{\nabla}u^{*}\cdot\vec{n})\vec{v}\,\mathrm{d}\Gamma$$

$$=\vec{n}(\xi)\cdot\int_{\Gamma}(\vec{\nabla}u^{*}\times\vec{n})\times\vec{v}\,\mathrm{d}\Gamma+\vec{n}(\xi)\int_{\Omega}(\vec{\omega}\times\vec{\nabla}u^{*})\,\mathrm{d}\Omega \tag{27}$$

Equations (26) and (27) basically represent the application of the boundary velocity conditions given for normal and tangential velocity components to the boundary.

For the closed cavity problem, where the boundary Γ represents the solid wall on which condition $\vec{v}=0$ is valid, then equation (24) reduces to

$$c(\xi)\vec{v}(\xi)=\int_{\Omega}(\vec{\omega}\times\vec{\nabla}u^{*})\,\mathrm{d}\Omega. \tag{28}$$

For such flow situations, the boundary integrals vanish, and the velocity field in the fluid domain is simply given by the domain integral of the vorticity field.

4.2 Integral representations for flow kinetics

Considering kinetics in an integral representation, one has to consider the parabolic diffusion-convection character of the vorticity transport equation (8). Since only the linear parabolic diffusion differential operator is employed, i.e.

$$\mathscr{L}[\cdot]=\nu\frac{\partial^{2}(\cdot)}{\partial x_{j}\partial x_{j}}-\frac{\partial(\cdot)}{\partial t}, \tag{29}$$

the vorticity equation can be formulated as a nonhomogeneous parabolic diffusion equation as follows

$$\mathscr{L}[\omega]+b=\nu\frac{\partial^{2}\omega}{\partial x_{j}\partial x_{j}}-\frac{\partial\omega}{\partial t}+b=0 \tag{30}$$

with the following corresponding integral representation written in a time increment form for a time step $\Delta t=t_{F}-t_{F-1}$:

$$c(\xi)\omega(\xi,t_{F})+\nu\int_{\Gamma}\int_{t_{F-1}}^{t_{F}}\omega\frac{\partial u^{*}}{\partial n}\,\mathrm{d}t\,\mathrm{d}\Gamma$$

$$=\nu\int_{\Gamma}\int_{t_{F-1}}^{t_{F}}\frac{\partial\omega}{\partial n}u^{*}\,\mathrm{d}t\,\mathrm{d}\Gamma+\int_{\Omega}\int_{t_{F-1}}^{t_{F}}bu^{*}\,\mathrm{d}t\,\mathrm{d}\Omega+\int_{\Omega}\omega_{F-1}u^{*}{}_{F-1}\,\mathrm{d}\Omega, \tag{31}$$

where u^{*} is the parabolic diffusion fundamental solution. The domain integral of the nonhomogeneous nonlinear contribution b, represented as

$$b = -\frac{\partial v_j \omega}{\partial x_j} + e_{ij} g_j \frac{\partial F_B}{\partial x_i}, \tag{32}$$

includes the convection and the buoyancy force term, thus the final integral statement reads as

$$\begin{aligned} c(\xi)\omega(\xi, t_F) + \nu \int_\Gamma \int_{t_{F-1}}^{t_F} \omega \frac{\partial u^*}{\partial n} \, \mathrm{d}t \, \mathrm{d}\Gamma \\ = \nu \int_\Gamma \int_{t_{F-1}}^{t_F} \frac{\partial \omega}{\partial n} u^* \, \mathrm{d}t \, \mathrm{d}\Gamma - \int_\Gamma \int_{t_{F-1}}^{t_F} \omega v_n u^* \, \mathrm{d}t \, \mathrm{d}\Gamma \\ + \int_\Omega \int_{t_{F-1}}^{t_F} \omega v_j \frac{\partial u^*}{\partial x_j} \, \mathrm{d}t \, \mathrm{d}\Omega + e_{ij} \int_\Gamma \int_{t_{F-1}}^{t_F} n_i g_j F_B u^* \, \mathrm{d}t \, \mathrm{d}\Gamma \\ - e_{ij} \int_\Omega \int_{t_{F-1}}^{t_F} g_j F_B \frac{\partial u^*}{\partial x_i} \, \mathrm{d}t \, \mathrm{d}\Omega + \int_\Omega \omega_{F-1} u^*_{F-1} \, \mathrm{d}\Omega. \end{aligned} \tag{33}$$

Equation (33) represents the vorticity transport in the integral form. Vorticity diffusion is described by the first two boundary integrals, the third boundary integral describes the convective flow on the boundary and the last boundary integral is due to vorticity generation on the boundary due to buoyancy forces. The first two domain integrals give the influence of forced and natural convection, while the last domain integral represents the initial vorticity distribution effect on the development of the vorticity field in the next time interval.

By applying a similar procedure to the heat transport equation (3), one derives the following integral statement

$$\begin{aligned} c(\xi)T(\xi, t_F) + a \int_\Gamma \int_{t_{F-1}}^{t_F} T \frac{\partial u^*}{\partial n} \, \mathrm{d}t \, \mathrm{d}\Gamma \\ = a \int_\Gamma \int_{t_{F-1}}^{t_F} \frac{\partial T}{\partial n} u^* \, \mathrm{d}t \, \mathrm{d}\Gamma - \int_\Gamma \int_{t_{F-1}}^{t_F} T v_n u^* \, \mathrm{d}t \, \mathrm{d}\Gamma \\ + \int_\Omega \int_{t_{F-1}}^{t_F} T v_j \frac{\partial u^*}{\partial x_j} \, \mathrm{d}t \, \mathrm{d}\Omega + \int_\Omega T_{F-1} u^*_{F-1} \, \mathrm{d}\Omega, \end{aligned} \tag{34}$$

where u^* is the parabolic diffusion fundamental solution.

5. Computational algorithm

If we want to obtain values of field functions in our computational domain, one has to first transform the derived integral equations into its discrete algebraic

forms, as presented by Hribersek and Skerget (1996), Skerget *et al.* (1999) and Wrobel (2002) among others. The key to this is division of computational external boundary into boundary elements and interior domain into domain cells. In the present work, quadratic interpolation functions were used in the case of boundary elements and internal cells.

Before we proceed to the description of computational procedure, let us first make a few remarks. The kinematics and kinetics of the fluid flow motion can be seen as two interlaced problems in a computational procedure. For general time dependent flows, using known information about the motion at an instant time level, new vorticity values for a subsequent time level are determined by solving the parabolic kinetic vorticity transport equation (8). With this new vorticity values, corresponding velocity values for subsequent time level are computed by solving the elliptic kinematic relation (7). These two related steps constitute a computational loop which advances the solution from initial level to a subsequent time level.

Additionally, due to the presence of buoyancy forces, the vorticity transport is also dependent on temperature distribution inside the fluid domain, which means that all the three equations are strongly coupled into a nonlinear system, which has to be solved iteratively.

The solution algorithm for the case of natural convection in closed cavities can therefore be written as:

(1) Choose initial vorticity (ω_0) and temperature (T_0) distributions, set $F = 0$, define the number of time steps NT.

(2) Time loop: $F = F + 1$

(3) Flow kinematics:

(3.1.) Solve equation (26) for boundary vorticities.

(3.2.) Compute domain velocities from equation (28) with $c(\xi) = 1$ explicitly.

(4) Energy transport:

Solve system (34) for unknown T and $\partial T/\partial n$.

(5) Vorticity transport:

(5.1.) Solve system (33) for unknown ω in the domain and $\partial \omega/\partial n$ on the boundary.

(5.2.) Use underrelaxation (Θ) for computing new domain vorticity values $(i + 1)$ for step 3.:

$$^{i+1}\{\omega\} = \Theta^{i+1}\{\omega\} + (1 - \Theta)\,^{i}\{\omega\}$$

(5.3.) Check convergence for predefined error ε (usually 0.0001, N_c = number of nodes):

$$C = \frac{\sum_{j=1}^{N_c} ({}^{i+1}\omega_j - {}^{i}\omega_j)^2}{\sum_{j=1}^{N_c} ({}^{i+1}\omega_j)^2}$$

If $C < \varepsilon$ go to 6.

If $C \geq \varepsilon$ go to 3.

(6) If $F < NT$ set $\{\omega\}_F = \{\omega\}_{F-1}$, $\{T\}_F = T\}_{F-1}$ and go to 2.

If $F \geq NT$ end.

6. Test problems

The presence of nonregular boundaries can significantly affect the thermal and flow conditions inside the cavity as compared with a square cavity. Two test cases were therefore selected to test the abilities of the developed numerical algorithm. In both test cases, there is a horizontal gradient of temperature, that causes onset of natural convection. Regarding the geometry, both geometry contractions and expansions are encountered. The selected test cases present an extension of the classical natural convection benchmark test of differentially heated square enclosure, performed by various authors, among others (Davis, 1983; Škerget *et al.*, 1989, 1999). In all cases, the Boussinesq approximation is employed to account for the thermal buoyancy effects, and the working fluid was air with $\mathrm{Pr} = 0.71$.

6.1 Natural convection in a heated backward facing step problem

The natural convection in a heated backward facing step can be seen as an extension of the classical natural convection in a closed cavity test. Here, this classical test case can be observed in the lower part of the cavity. The test configuration is shown in Figure 1. The backward step wall is heated and kept at a constant temperature T_1, while the right wall is cooled and kept at a lower temperature T_2, all other walls are adiabatic.

In comparison with square cavity test, the upper wall of the square cavity is replaced here by a large horizontal cavity, which significantly affects the temperature and flow field in the upper part of the cavity.

Computational mesh, shown in Figure 2, consisted of 96 quadratic boundary elements and 432 internal cells in a 24×24 mesh pattern with element ratio 4.The computational mesh was therefore denser near the solid walls, where large gradients in temperature and velocity profiles were expected.

The computations were performed for Ra number values in the range $10^2 - 10^5$. Here, Rayleigh number value was defined as (h stands for the height of the heated backward step wall, i.e. 0.5),

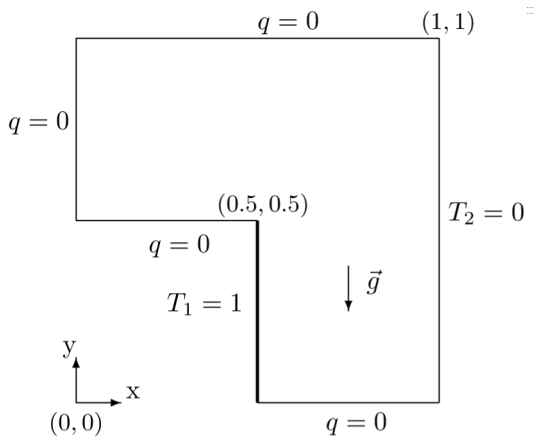

Figure 1.
Presentation of the heated backward facing step problem

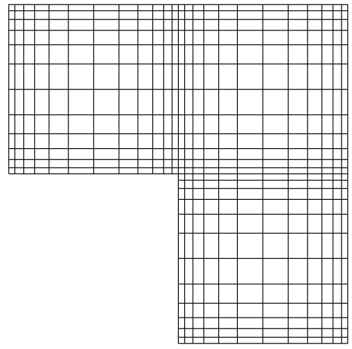

Figure 2.
Computational mesh for L domain: 24×24 cells with ratio 4

$$\mathrm{Ra} = \frac{g\beta(T_1 - T_2)h^3}{\nu a}. \tag{35}$$

From the results in Figures 3 and 4 we see the effect of the expansion of the cavity in the upper half. Whereas isotherms are quite close to the ones in a square cavity, in the upper part a strong recirculation due to abrupt increase in cavity width is formed. This is the cause of dominance of convective heat transfer in the upper part of the cavity, especially evident in the case of $\mathrm{Ra} = 10^5$ (Figure 4).

In order to compare our results with the results of computations of Chang and Tsay (2001), where 80×80 finite difference mesh was used, average Nu number values were computed as

$$\overline{\mathrm{Nu}} = -\int_0^1 \left(\frac{\partial T}{\partial n}\right)_{x=1} \mathrm{d}y. \tag{36}$$

Figure 5 shows the obtained results together with the results of Chang and Tsay (2001) and CFX (2001). Also, computations with CFX-4 CFD software were performed on 80×80 mesh. It is also interesting to see the difference in Nu numbers when compared with classical square cavity test. This comparison is shown in Figure 6 with *bem nc* results for square cavity obtained by boundary domain integral method from Hribersek and Skerget (1996). Due to the expansion in the cavity the local velocities near the point (0.5,0.5) increase as compared with a square cavity, increasing also local heat transfer rate and resulting in a higher average Nu number value.

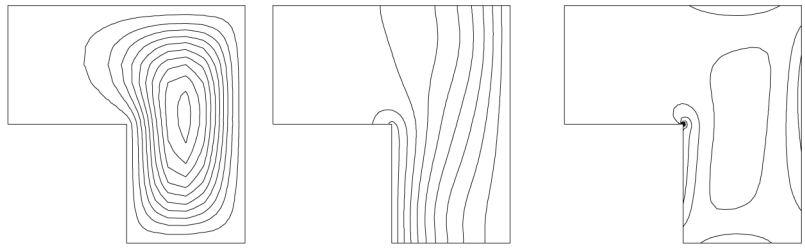

Figure 3.
Contour plots of streamlines, temperatures and vorticities for $Ra = 10^3$

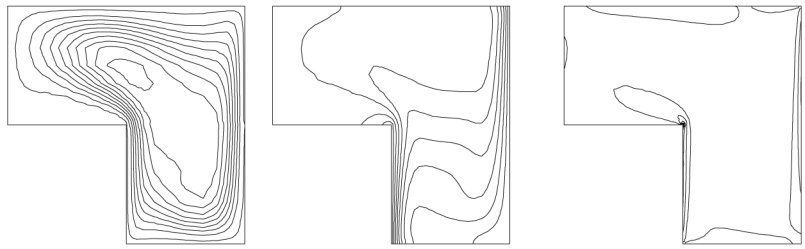

Figure 4.
Contour plots of streamlines, temperatures and vorticities for $Ra = 10^5$

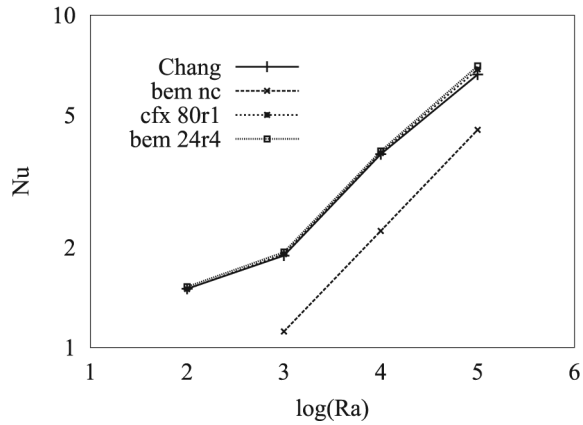

Figure 5.
Average Nusselt number for different values of Ra number (bem 24 – current computations, bem nc – computations in Hribersek and Skerget (1996)

6.2 Natural convection in a H shaped cavity

The second test case selected can also be seen as a derivation of a standard square cavity test, but in this case there are additional solid wall partitions, that protrude centrally from the top and bottom walls into the cavity. The test configuration is presented in Figure 6. The partition length is one quarter of the cavity height, h. The Rayleigh number is defined as in equation (35). Computational mesh used consisted of 100 boundary elements and 380 internal cells (Figure 7).

As the effect of partitions on heat transfer is more pronounced at lower Ra number values (Ciofalo and Karayiannis, 1991), computations were performed for Ra number values between 10^3 and 3.5×10^5. From the computational results, shown in Figures 8-10, partitions reduce the fluid flow along the isothermal walls and thus reduce also the heat transfer rate at the walls. This is also evident from the comparison of average Nu number values of present calculation and calculation for square cavity problem with the presented BEM algorithm, shown in Table I. Comparison with results of finite volume method of CFX-4, where computations were performed on 64×64 mesh, shows very

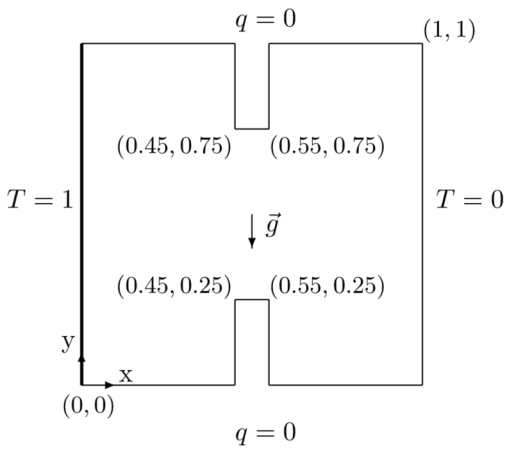

Figure 6.
Presentation of the H shaped cavity problem

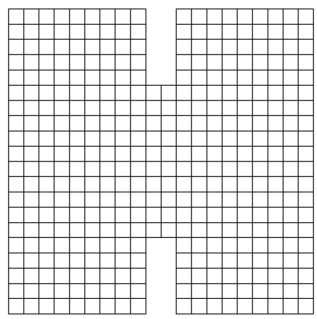

Figure 7.
Computational mesh for H shaped cavity: 20×20 cells

good agreement. Note that contours of streamlines are post processing results, calculated outside the BEM algorithm.

7. Conclusions

Boundary-domain integral approach to the solution of natural convection problems is considered. The accuracy of the presented numerical algorithm is shown on numerical modelling of several complex geometries of closed cavity problems. The results for relatively coarse meshes are accurate as shown by the comparison with available numerical data of other authors.

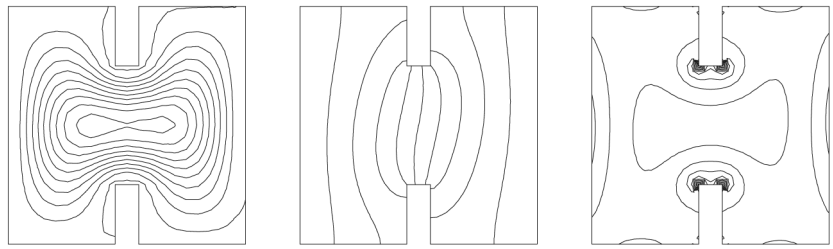

Figure 8.
Contour plots of streamlines, temperatures and vorticities for $Ra = 10^3$

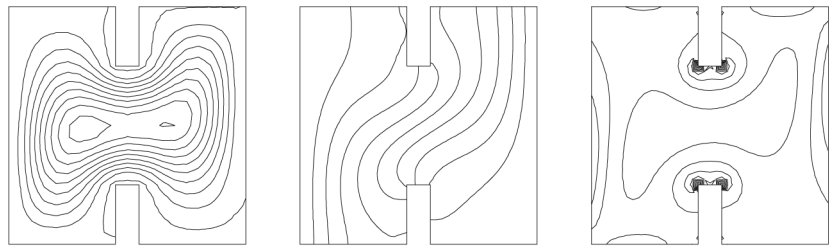

Figure 9.
Contour plots of streamlines, temperatures and vorticities for $Ra = 10^4$

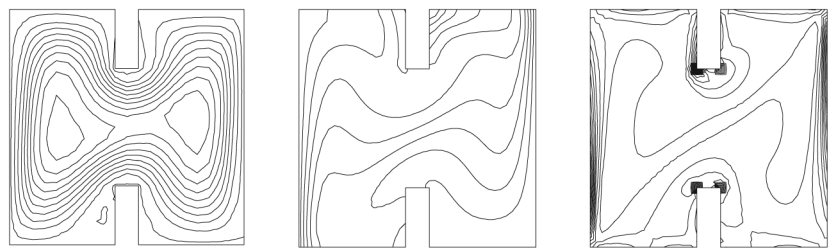

Figure 10.
Contour plots of streamlines, temperatures and vorticities for $Ra = 3.5 \times 10^5$

Table I.
Comparison of average Nu numbers for H shaped cavity and square cavity

Nusselt number	Rayleigh number 10^3	10^4	3.5×10^5
H cavity (present)	0.753	1.231	6.025
H cavity (CFX, 2001)	0.751	1.267	6.065
Square cavity (present)	1.118	2.243	6.582

The solution algorithm is based on the velocity-vorticity formulation of the Navier-Stokes equations. The kinematics is given by the Poisson velocity equation, while the kinetics is considered in a form of vorticity transport equation. It is shown that the integral representation for the velocity equation is identical to the one based on Poisson vector potential equation, when additional restriction conditions are applied. This formulation ensures the solenoidality of the velocity and vorticity fields for general flow problems.

The unique ability of the integral representation approach is based on the use of Green functions, thus the linear part of the transport phenomena is described by the boundary integrals only, while the nonlinear effects are modelled by the internal domain discretization. The critical part of the kinematics, the computation of boundary vorticity values, is done in a global integral manner, establishing the method superior to the other domain type numerical models. It should be mentioned that the introduction of the segmentation technique (Hribersek and Skerget, 1996), for the flow kinematics and the subdomain technique (Skerget *et al.*, 1999) for the kinetics presents another very promising direction of the development of the proposed method, especially when computation of large engineering problems should be considered.

References

CFX 4.4 (2001), AEA Technology.

Chang, T.S. and Tsay, Y.L. (2001), "Natural convection in an enclosure with a heated backward step", *Int. J. Heat and Mass Transfer*, Vol. 44, pp. 3963-71.

Ciofalo, M. and Karayiannis, T.G. (1991), "Natural convection heat transfer in a partially – or completely partitioned vertical enclosure", *Int. J. Heat and Mass Transfer*, Vol. 34, pp. 167-79.

Davis, G.D.V. (1983), "Natural convection of air in a square cavity: a bench mark numerical solution", *Int. J. for Num. Meth. in Fluids*, Vol. 3, pp. 249-64.

Hribersek, M. and Kuhn, G. (2000), "Conjugate heat transfer by boundary-domain integral method", *Eng. Anal. Bound. Elem.*, Vol. 24, pp. 297-305.

Hribersek, M. and Skerget, L. (1996), "Iterative methods in solving Navier-Stokes equations by the boundary element method", *Int. J. Num. Meth. Eng.*, Vol. 39, pp. 115-39.

Škerget, L., Hriberťek, M. and Kuhn, G. (1999), "Computational fluid dynamics by boundary domain integral method", *Int. J. Num. Meth. Eng.*, Vol. 46, pp. 1291-311.

Skerget, L., Alujevic, A., Brebbia, C.A. and Kuhn, G. (1989), "Natural and forced convection simulation using the velocity-vorticity approach", *Topics in Boundary Element Research*, Vol. 5, Springer-Verlag, Berlin, pp. 49-86.

Wrobel, L.C. (2002), *The Boundary Element Method*, Applications in Thermo-fluids and acoustics, Vol. 1, Wiley, NY.

Wu, J.C. (1982), "Problems of general viscous fluid flow", *Developments in BEM*, Ch. 2. Vol. 2, Elsevier, London and NY.

Wu, J.C. and Thompson, J.F. (1973), "Numerical solution of time dependent incompressible Navier-Stokes equations using an integro-differential formulation", *Comp. and Fluids*, Vol. 1, pp. 197-215.